Coordination Modes of a Series of Xylylene-Bridged Bis(1,4,7-triazacyclonon-1-yl) Ligands: Synthesis, Structure, and Properties of Nickel(II) and Copper(II) Complexes

Bim Graham,[†] Gary D. Fallon,[†] Milton T. W. Hearn,[‡] David C. R. Hockless,[§] George Lazarev,[†] and Leone Spiccia*[,†]

Department of Chemistry, Monash University, Clayton, Victoria 3168, Australia, Centre for Bioprocess Technology, Department of Biochemistry and Molecular Biology, Monash University, Victoria 3168, Australia, and Research School of Chemistry, Australian National University, Canberra, ACT 0200, Australia

Received May 30, 1997[⊗]

Three bis(1,4,7-triazacyclonon-1-yl) ligands, 1,2-bis(1,4,7-triazacyclonon-1-ylmethyl)benzene (L^1), 1,3-bis(1,4,7-triazacyclonon-1-ylmethyl)benzene (L^2), and 1,4-bis(1,4,7-triazacyclonon-1-ylmethyl)benzene (L^3), have been synthesized and their nickel(II) and copper(II) coordination chemistry investigated. Reaction of L^1 with excess Ni^{2+} ions affords a mixture of mononuclear and binuclear complexes, which are readily separated by cation exchange chromatography and crystallized as their perchlorate salts, $[NiL^1](ClO_4)_2$ (**1**) and $[Ni_2L^1(H_2O)_6](ClO_4)_4 \cdot 4H_2O$ (**2**). Similar treatment of L^2 and L^3 with excess Ni^{2+} ions affords exclusively the binuclear complexes $[Ni_2L^2(H_2O)_6](ClO_4)_4$ (**3**) and $[Ni_2L^3(H_2O)_6](ClO_4)_4 \cdot 3H_2O$ (**4**), respectively. Reaction of all three ligands with excess Cu^{2+} ions also yields binuclear complexes, which may be isolated as neutral species, $[Cu_2LBr_4] \cdot x$DMF (**5**, L = L^1, $x = 1$; **6**, L = L^2, $x = 0$; **7**, L = L^3, $x = 0$), or as perchlorate salts, $[Cu_2L(H_2O)_4](ClO_4)_4 \cdot xH_2O$ (**8**, L = L^1, $x = 5$; **9**, L = L^2, $x = 4$; **10**, L = L^3, $x = 5$). The mononuclear copper(II) complex of L^1 is prepared by reaction of L^1 with Cu^{2+} ions in a 1:1 mole ratio and isolated as its perchlorate salt, $[CuL^1](ClO_4)_2 \cdot 2H_2O$ (**11**). The X-ray structures of complexes **1**·H_2O, **4**, **5**, and **11** have been determined. Compound **1**·H_2O crystallizes in the monoclinic space group $P2_1/c$ (No. 14) with $a = 9.212(3)$ Å, $b = 17.805(8)$ Å, $c = 16.501(6)$ Å, $\beta = 103.36(3)°$, $V = 2633(1)$ Å^3, and $Z = 4$; **4**, in the monoclinic space group $P2_1/c$ (No. 14) with $a = 9.108(4)$ Å, $b = 25.857(5)$ Å, $c = 17.524(2)$ Å, $\beta = 92.73(2)°$, $V = 4122(2)$ Å^3, and $Z = 4$; **5**, in the trigonal space group $P3_121$ (No. 152) with $a = 10.889(5)$ Å, $c = 22.220(9)$ Å, $V = 2281(1)$ Å^3, and $Z = 3$; and **11**, in the monoclinic space group $P2_1/c$ (No. 14) with $a = 9.45(1)$ Å, $b = 19.51(2)$ Å, $c = 15.10(1)$ Å, $\beta = 96.93(8)°$, $V = 2763(4)$ Å^3, and $Z = 4$. The nickel(II) and copper(II) centers in the mononuclear complexes, **1**·H_2O and **11**, lie in distorted octahedral environments, sandwiched by the two facially coordinating triamine rings of L^1. In complex **4**, the two triamine rings of L^3 coordinate to separate nickel(II) centers, with the distorted octahedral coordination sphere about each of the metal centers being completed by water molecules. Similarly, in complex **5**, the two triamine rings of L^1 bind separate copper(II) centers, with the distorted square pyramidal coordination sphere about each of the metal centers being completed by bromide anions.

Introduction

The design and metal complexation properties of ligands constructed by linking 1,4,7-triazacyclononane (tacn) macrocycles have become the focus of considerable research activity since Takamoto and co-workers[1] reported the first example, incorporating an ethane linker, two decades ago. To date, bis(tacn) compounds linked by alkane,[1−8] alcohol,[9] ether,[3] phenol,[10] pyrazole,[11] naphthalene,[12] and calixarene[13] units have been prepared. In a few cases, these have been further structurally elaborated through functionalization with potentially coordinating pendant arms.[14−16]

Takamoto and co-workers[1] recognized the mononucleating potential of their ligand, reporting the synthesis of a series of complexes believed to have sandwich-type structures, in which the two tacn rings simultaneously coordinate to a single metal ion. Most of the current interest in bis(tacn) compounds, however, stems from their potential ability to facially coordinate to two separate metal centers, forming binuclear (or higher nuclearity) complexes, while leaving coordination sites available for the attachment of additional ligands. Some of the resulting

[†] Department of Chemistry, Monash University.
[‡] Centre for Bioprocess Technology, Monash University.
[§] Australian National University.
[⊗] Abstract published in *Advance ACS Abstracts,* December 15, 1997.

(1) Tanaka, N.; Kobayashi, Y.; Takamoto, S. *Chem. Lett.* **1977**, 107.
(2) Wieghardt, K.; Tolksdorf, I.; Herrmann, W. *Inorg. Chem.* **1985**, *24*, 1230.
(3) Weisman, G. R.; Vachon, D. J.; Johnson, V. B.; Gronbeck, D. A. *J. Chem. Soc., Chem. Commun.* **1987**, 886.
(4) Geilenkirchen, A.; Wieghardt, K.; Nuber, B.; Weiss, J. *Z. Naturforsch.* **1989**, *44B*, 1333.
(5) Sessler, J. L.; Sibert, J. W.; Lynch, V. *Inorg. Chem.* **1990**, *29*, 4143.
(6) Sessler, J. L.; Sibert, J. W.; Burrell, A. K.; Lynch, V.; Markert, J. T.; Wooten, C. L. *Inorg. Chem.* **1993**, *32*, 621.
(7) Hanke, D.; Wieghardt, K.; Nuber, B.; Lu, R.-S.; McMullan, R. K.; Koetzie, T. F.; Bau, R. *Inorg. Chem.* **1993**, *32*, 4300.
(8) Zhang, X.; Hsieh, W.-Y.; Margulis, T. N.; Zompa, L. J. *Inorg. Chem.* **1995**, *34*, 2883.
(9) Sessler, J. L.; Sibert, J. W.; Burrell, A. K.; Lynch, V.; Markert, J. T.; Wooten, C. L. *Inorg. Chem.* **1993**, *32*, 4277.
(10) Chang, H.; Diril, H.; Nilges, M. J.; Zhang, X.; Potenza, J. A.; Schugar, H. J.; Hendrickson, D. N.; Isied, S. S. *J. Am. Chem. Soc.* **1988**, *110*, 625.
(11) Behle, L.; Neuburger, M.; Zehnder, M.; Kaden, T. A. *Helv. Chim. Acta* **1995**, *78*, 693.
(12) Young, M. J.; Chin, J. *J. Am. Chem. Soc.* **1995**, *117*, 10577.
(13) Beer, P. D.; Drew, M. G. B.; Leeson, P. B.; Lyssenko, K.; Ogden, M. I. *J. Chem. Soc., Chem. Commun.* **1995**, 929.
(14) Blake, A. J.; Donlevy, T. M.; England, P. A.; Fallis, I. A.; Parsons, S.; Schröder, M. *J. Chem. Soc., Chem. Commun.* **1994**, 1981.
(15) Brudenell, S. J.; Spiccia, L.; Tiekink, E. R. T. *Inorg. Chem.* **1996**, *35*, 1974.
(16) Fry, F. H.; Graham, B.; Spiccia, L.; Hockless, D. C. R.; Tiekink, E. R. T. *J. Chem. Soc., Dalton Trans.* **1997**, 827.

S0020-1669(97)00642-3 CCC: $14.00 © 1997 American Chemical Society

Chart 1

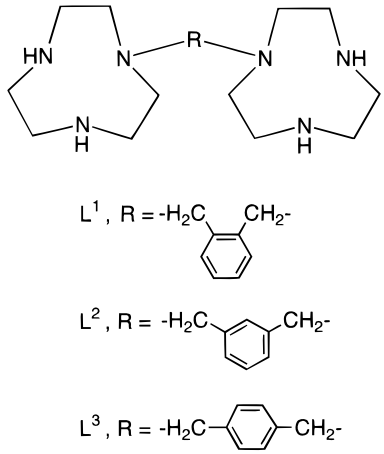

complexes have been found to model the active sites of metalloproteins,[2,5,6,9,10] while others have found application as catalytic reagents which function through the concerted action of two metal centers[12] and in the study of magnetic exchange interactions between paramagnetic metal centers.[6,9−11,13,15]

Our own interest in bis(tacn) complexes is as receptors for substrates bearing two potentially coordinating groups. Through appropriate choice of the group bridging the two tacn macrocycles, we envisage that it should be possible to construct binuclear complexes in which the metal−metal distance is complementary to the distance between the two coordinating groups, permitting strong two-point binding of the substrate. With a certain degree of rigidity in the bridging unit, selectivity for the given substrate over similar compounds might also be expected. Toward this end we have synthesized a series of bis(tacn) ligands (Chart 1), incorporating *o*-, *m*-, and *p*-xylylene bridging groups, in which the distance between the two macrocycles is systematically varied, and we are examining the coordination chemistry of these ligands. Reported here are the structures and properties of nickel(II) and copper(II) complexes of these ligands.

Experimental Section

Materials and Reagents. Reagent or analytical grade materials were obtained from commercial suppliers and used without further purification. 1,4,7-Triazatricyclo[5.2.1.$0^{4,10}$]decane was prepared from 1,4,7-triazacyclononane by a published method.[8]

Physical Measurements. Proton and carbon NMR spectra were recorded for D_2O solutions on a Bruker AC200 spectrometer and are referenced to an internal standard of sodium 3-(trimethylsilyl)propionate-*2,2,3,3-d*$_4$ and an external standard of tetramethylsilane, respectively. Infrared spectra were recorded on a Perkin-Elmer 1600 FTIR spectrophotometer as KBr pellets or Nujol mulls, and electronic spectra, on a Cary 3 or Cary 5 spectrophotometer. Electron microprobe analyses were made with a JEOL JSM-1 scanning electron microscope through an NEC X-ray detector and pulse-processing system connected to a Packard multichannel analyzer. Microanalyses were performed by the Chemical and Micro-Analytical Services (CMAS), Melbourne, Australia. Room-temperature magnetic moments were determined by the Faraday method. Diamagnetic corrections were made using Pascal's constants. ESR spectra were recorded on a Varian E-12 spectrometer as frozen (77 K) DMF solutions and simulated with the aid of the Bruker Simfonia program.

Caution! *Although no problems were encountered in this work, perchlorate salts of transition metal complexes are potentially explosive and should thus be prepared in small quantities and handled with due care.*

Hexahydrobromide Salts of 1,2-, 1,3-, and 1,4-Bis(1,4,7-triazacyclonon-1-ylmethyl)benzene (L^1·6HBr·1.5H_2O, L^2·6HBr·1.5H_2O, and L^3·6HBr·3.5H_2O). A solution of 1,2-, 1,3-, or 1,4-bis(bromomethyl)benzene (1.42 g, 5.38 mmol) in dry acetonitrile (50 mL) was added dropwise to a stirred solution of 1,4,7-triazatricyclo[5.2.1.$0^{4,10}$]-decane (1.50 g, 10.8 mmol) in dry acetonitrile (50 mL) over a period of 2 h. The white precipitate which formed during the addition was filtered off, washed with dry acetonitrile (10 mL), and dried in a vacuum desiccator. The solid was then dissolved in distilled water (25 mL), and the solution was refluxed for 3 h. Sodium hydroxide pellets (2.00 g, 50 mmol) were carefully added in portions to the solution, and refluxing was continued for a further 4 h. After cooling to room temperature, the solution was extracted with chloroform (4 × 100 mL), the combined extracts were dried over magnesium sulfate, and the solvent was removed under reduced pressure to yield a pale yellow oil. This was dissolved in distilled water (5 mL) and concentrated hydrobromic acid (50 mL) added dropwise to afford a white precipitate. Recrystallization of the precipitate from a mixture of water and concentrated hydrobromic acid yielded the pure product as a white microcrystalline solid.

L^1·6HBr·1.5H_2O: yield 3.51 g, 75%. Anal. Calcd for $C_{20}H_{45}Br_6N_6O_{1.5}$ (L^1·6HBr·1.5H_2O): C, 27.5; H, 5.2; N, 9.6. Found: C, 27.6; H, 5.2; N, 9.4. ^{1}H NMR: δ 3.09 (8H, t, tacn ring CH_2), 3.26 (8H, t, tacn ring CH_2), 3.72 (8H, s, tacn ring CH_2), 4.11 (4H, s, bridge CH_2), 7.48 (2H, m, aromatic CH), 7.63 (2H, m, aromatic CH). ^{13}C NMR: δ 42.56, 44.12, 48.54 (tacn ring CH_2), 56.07 (bridge CH_2), 128.64, 131.53 (aromatic CH), 135.20 (aromatic quaternary C).

L^2·6HBr·1.5H_2O: yield 3.00 g, 64%. Anal. Calcd for $C_{20}H_{45}Br_6N_6O_{1.5}$ (L^2·6HBr·1.5H_2O): C, 27.5; H, 5.2; N, 9.6. Found: C, 27.6; H, 5.5; N, 9.4. ^{1}H NMR: δ 3.06 (8H, t, tacn ring CH_2), 3.28 (8H, t, tacn ring CH_2), 3.66 (8H, s, tacn ring CH_2), 3.99 (4H, s, bridge CH_2), 7.49 (4H, br, aromatic CH). ^{13}C NMR: δ 42.06, 43.53, 47.33 (tacn ring CH_2), 58.42 (bridge CH_2), 129.12, 130.02, 131.91 (aromatic CH), 135.59 (aromatic quaternary C).

L^3·6HBr·3.5H_2O: yield 3.11 g, 64%. Anal. Calcd for $C_{20}H_{49}Br_6N_6O_{3.5}$ (L^3·6HBr·3.5H_2O): C, 26.4; H, 5.4; N, 9.2. Found: C, 26.7; H, 5.3; N, 8.9. ^{1}H NMR: δ 3.09 (8H, t, tacn ring CH_2), 3.27 (8H, t, tacn ring CH_2), 3.69 (8H, s, tacn ring CH_2), 3.98 (4H, s, bridge CH_2), 7.51 (4H, s, aromatic CH). ^{13}C NMR: δ 42.00, 43.41, 47.30 (tacn ring CH_2), 58.31 (bridge CH_2), 130.61 (aromatic CH), 134.85 (aromatic quaternary C).

$[NiL^1](ClO_4)_2$ (1) and $[Ni_2L^1(H_2O)_6](ClO_4)_4$·4$H_2O$ (2). To an aqueous solution (50 mL) of $Ni(NO_3)_2$·6H_2O (1.03 g, 3.54 mmol) and L^1·6HBr·1.5H_2O (1.00 g, 1.15 mmol), heated on a steam bath, was added sodium hydroxide solution (2 M) until a small amount of nickel hydroxide precipitate appeared which would not dissolve on heating. Sufficient dilute hydrochloric acid (2 M) was then added to just dissolve this precipitate and the resulting pink-purple solution heated for a further 15 min before being diluted to 2 L with distilled water and loaded onto a Sephadex SP-C25 cation-exchange column (H^+ form, 15 cm × 4 cm). After washing with distilled water and 0.1 M sodium perchlorate solution, a pink band and a light green band (excess Ni^{2+}) were eluted from the column with 0.3 M sodium perchlorate solution. The pink fraction yielded pink crystals of **1** within 30 min, which were filtered off, washed with methanol, and air-dried. Yield: 0.15 g, 21%. Anal. Calcd for $C_{20}H_{36}Cl_2N_6NiO_8$ ($[NiL^1](ClO_4)_2$): C, 38.9; H, 5.9; N, 13.6. Found: C, 38.8; H, 6.1; N, 13.7. Electron microprobe: Ni and Cl uniformly present. UV−visible spectrum (CH_3CN): λ_{max}, nm (ϵ_{max}) = 340 (sh), 359 (7), 538 (7), ∼625 (sh), ∼840 (sh), 912 (16). Selected IR bands (KBr, cm^{-1}): 3419 s, br, 3206 m, 2931 w, 1638 s, 1620 s, 1492 m, 1147 s, 1117 s, 1080 s, 627 s. Magnetic moment: μ_{eff}(293 K) = 3.01 μ_B. Slow evaporation of an aqueous solution of **1** gave crystals of **1**·H_2O suitable for X-ray crystallography.

A third band, pale purple-blue in color, was eluted from the Sephadex column using 0.8 M sodium perchlorate solution. Slow evaporation of this fraction over a number of days yielded pale purple-blue crystals of **2**, which were filtered off and air-dried. Prior to analysis, the solid was washed quickly with a small amount of cold methanol. This purification step resulted in considerable loss of product. Yield: 0.36 g, 30%. Anal. Calcd for $C_{20}H_{56}Cl_4N_6Ni_2O_{26}$ ($[Ni_2L^1(H_2O)_6](ClO_4)_4$·4$H_2O$): C, 22.7; H, 5.3; N, 8.0. Found: C, 22.4; H, 4.8; N, 8.0. Electron microprobe: Ni and Cl uniformly present. UV−visible spectrum (water): λ_{max}, nm (ϵ_{max}) = 356 (13), 578 (9), ∼775 (sh), 978 (30). Selected IR bands (Nujol, cm^{-1}): 3423 s, br, 3314 s, 1637 s, br, 1087 s, br, 623 s. Selected IR bands (KBr, cm^{-1}): 3475 s, br, 3320 s, 2979 w, 1639 s, br, 1495 m, 1098 s, br, 625 s. Magnetic moment: μ_{eff}(292 K) = 2.98 μ_B per nickel(II).

$[Ni_2L^2(H_2O)_6](ClO_4)_4$ (3) and $[Ni_2L^3(H_2O)_6](ClO_4)_4 \cdot 3H_2O$ (4). Treatment of an aqueous solution (50 mL) of $Ni(NO_3)_2 \cdot 6H_2O$ (1.03 g, 3.54 mmol) and $L^2 \cdot 6HBr \cdot 1.5H_2O$ (1.00 g, 1.15 mmol) or $L^3 \cdot 6HBr \cdot 3.5H_2O$ (1.00 g, 1.10 mmol) as described above afforded a blue solution, which was again loaded onto a Sephadex SP-C25 cation-exchange column. Following elution of a light green band of excess Ni^{2+} with 0.3 M sodium perchlorate solution, only one other band, purple-blue in color, was eluted from the column, using 0.8 M sodium perchlorate solution. Slow evaporation of this fraction yielded pale purple-blue crystals, which were filtered off and air-dried.

3: yield 0.49 g, 43%. Anal. Calcd for $C_{20}H_{48}Cl_4N_6Ni_2O_{22}$ ($[Ni_2L^2(H_2O)_6](ClO_4)_4$): C, 24.4; H, 4.9; N, 8.5. Found: C, 24.4; H, 4.8; N, 8.4. Electron microprobe: Ni and Cl uniformly present. UV−visible spectrum (water): λ_{max}, nm (ϵ_{max}) = 358 (11), 579 (8), ~775 (sh), 972 (32). Selected IR bands (Nujol, cm^{-1}): 3495 s, br, 3317 s, 1636 s, br, 1090 s, br, 624 s. Selected IR bands (KBr, cm^{-1}): 3476 s, br, 3322 s, 2952 w, 1649 s, br, 1493 m, 1092 s, br, 626 s. Magnetic moment: μ_{eff}(292 K) = 2.94 μ_B per nickel(II).

4: yield 0.43 g, 38%. Anal. Calcd for $C_{20}H_{54}Cl_4N_6Ni_2O_{25}$ ($[Ni_2L^3(H_2O)_6](ClO_4)_4 \cdot 3H_2O$): C, 23.1; H, 5.2; N, 8.1. Found: C, 22.7; H, 5.0; N, 8.0. Electron microprobe: Ni and Cl uniformly present. UV−visible spectrum (water): λ_{max}, nm (ϵ_{max}) = 357 (11), 581 (9), ~775 (sh), 973 (35). Selected IR bands (Nujol, cm^{-1}): 3448 s, br, 3314 s, 1638 s, br, 1102 s, br, 624 s. Selected IR bands (KBr, cm^{-1}): 3477 s, br, 3326 s, 2952 w, 1639 s, br, 1494 m, 1104 s, br, 625 s. Magnetic moment: μ_{eff}(292 K) = 2.96 μ_B per nickel(II). Crystals of **4** proved suitable for X-ray crystallography.

$[Cu_2L^1Br_4] \cdot DMF$ (5), $[Cu_2L^2Br_4]$ (6), and $[Cu_2L^3Br_4]$ (7). $CuBr_2$ (0.20 g, 0.90 mmol) and $L^1 \cdot 6HBr \cdot 1.5H_2O$ (0.30 g, 0.34 mmol), $L^2 \cdot 6HBr \cdot 1.5H_2O$ (0.30 g, 0.34 mmol), or $L^3 \cdot 6HBr \cdot 3.5H_2O$ (0.30 g, 0.33 mmol) were dissolved in distilled H_2O (100 mL), and sodium hydroxide solution (1 M) was added dropwise until a small amount of copper hydroxide precipitate appeared. Dilute hydrobromic acid (2 M) was then added dropwise to just dissolve this precipitate. The resulting dark blue solution was left to slowly evaporate, yielding a green powder. Recrystallization from a DMF/H_2O mixture yielded green crystals.

5: yield 0.17 g, 56%. Anal. Calcd for $C_{23}H_{43}Br_4Cu_2N_7O$ ($Cu_2L^1Br_4 \cdot DMF$): C, 31.4; H, 4.9; N, 11.1. Found: C, 31.3; H, 4.9; N, 11.1. Electron microprobe: Cu and Br uniformly present. Selected IR bands (KBr, cm^{-1}): 3294 s, 2939 m, 1676 vs, 1443 m, 1357 m, 1088 s, 935 s. Magnetic moment: μ_{eff}(291 K) = 1.87 μ_B per copper(II). Crystals of **5** proved suitable for X-ray crystallography.

6: yield 0.21 g, 76%. Anal. Calcd for $C_{20}H_{36}Br_4Cu_2N_6$ ($Cu_2L^2Br_4$): C, 29.8; H, 4.5; N, 10.4. Found: C, 29.9; H, 4.5; N, 10.4. Electron microprobe: Cu and Br uniformly present. Selected IR bands (KBr, cm^{-1}): 3238 s, 2922 w, 1449 m, 1352 m, 1092 s, 937 s. Magnetic moment: μ_{eff}(291 K) = 1.82 μ_B per copper(II).

7: yield 0.15 g, 56%. Anal. Calcd for $C_{20}H_{36}Br_4Cu_2N_6$ ($Cu_2L^3Br_4$): C, 29.8; H, 4.5; N, 10.4. Found: C, 29.8; H, 4.5; N, 10.5. Electron microprobe: Cu and Br uniformly present. Selected IR bands (KBr, cm^{-1}): 3253 s, 2926 m, 1450 m, 1350 m, 1097 s, 942 s. Magnetic moment: μ_{eff}(291 K) = 1.87 μ_B per copper(II).

$[Cu_2L^1(H_2O)_4](ClO_4)_4 \cdot 5H_2O$ (8), $[Cu_2L^2(H_2O)_4](ClO_4)_4 \cdot 4H_2O$ (9), and $[Cu_2L^3(H_2O)_4](ClO_4)_4 \cdot 5H_2O$ (10). To a solution of $Cu(NO_3)_2 \cdot 3H_2O$ (0.64 g, 2.7 mmol) and $L^1 \cdot 6HBr \cdot 1.5H_2O$ (1.00 g, 1.15 mmol), $L^2 \cdot 6HBr \cdot 1.5H_2O$ (1.00 g, 1.15 mmol), or $L^3 \cdot 6HBr \cdot 3.5H_2O$ (1.00 g, 1.10 mmol) dissolved in distilled H_2O (50 mL) was added sodium hydroxide solution (2 M) until a precipitate of copper hydroxide began to appear. Sufficient dilute hydrochloric acid (2 M) to just dissolve this precipitate was then added. The resulting dark blue solution was diluted to 2 L with distilled H_2O and loaded onto a Sephadex SP-C25 cation-exchange column (H^+ form, 15 cm × 4 cm). After the column was washed with distilled water and 0.2 M sodium perchlorate solution to remove a light green band of excess Cu^{2+}, a blue band was eluted with 0.6 M sodium perchlorate solution. This fraction was concentrated to about 50 mL on a rotary evaporator and then left to slowly evaporate. Blue crystals of the product formed, which were filtered off and air-dried. Prior to analysis the solid was washed quickly with a small amount of cold methanol. This purification step resulted in considerable loss of product.

8: yield 0.62 g, 52%. Anal. Calcd for $C_{20}H_{54}Cl_4Cu_2N_6O_{25}$ ($[Cu_2L^1(H_2O)_4](ClO_4)_4 \cdot 5H_2O$): C, 22.9; H, 5.2; N, 8.0. Found: 22.9; H, 5.0; N, 8.0. Electron microprobe: Cu and Cl uniformly present. UV−visible spectrum (water): λ_{max}, nm (ϵ_{max}) = 655 (79), 1056 (35). Selected IR bands (Nujol, cm^{-1}): 3500 br, 3300 m, 1636 br, 1491 m, 1356 m, 1082 s, 622 s. Magnetic moment: μ_{eff}(291 K) = 1.76 μ_B per copper(II).

9: yield 0.74 g, 63%. Anal. Calcd for $C_{20}H_{52}Cl_4Cu_2N_6O_{24}$ ($[Cu_2L^2(H_2O)_4](ClO_4)_4 \cdot 4H_2O$): C, 23.3; H, 5.1; N, 8.2. Found: C, 23.2; H, 5.1; N, 8.0. Electron microprobe: Cu and Cl uniformly present. UV−visible spectrum (water): λ_{max}, nm (ϵ_{max}) = 645 (72), 1044 (35). Selected IR bands (Nujol, cm^{-1}): 3500 br, 3293 s, 1636 br, 1490 m, 1353 m, 1092 s, 622 s. Magnetic moment: μ_{eff}(291 K) = 1.82 μ_B per copper(II).

10: yield 0.56 g, 49%. Anal. Calcd for $C_{20}H_{54}Cl_4Cu_2N_6O_{25}$ ($[Cu_2L^3(H_2O)_4](ClO_4)_4 \cdot 5H_2O$): C, 22.9; H, 5.2; N, 8.0. Found: C, 22.8; H, 5.0; N, 7.8. Electron microprobe: Cu and Cl uniformly present. UV−visible spectrum (water): λ_{max}, nm (ϵ_{max}) = 649 (70), 1050 (35). Selected IR bands (Nujol, cm^{-1}): 3500 br, 3294 s, 1616 br, 1490 m, 1355 m, 1090 s, 623 s. Magnetic moment: μ_{eff}(290 K) = 1.84 μ_B per copper(II).

$[CuL^1](ClO_4)_2 \cdot 2H_2O$ (11). To a solution of $Cu(NO_3)_2 \cdot 3H_2O$ (0.015 g, 0.062 mmol) and $L^1 \cdot 6HBr \cdot 1.5H_2O$ (0.055 g, 0.063 mmol) dissolved in distilled H_2O (20 mL) was added sodium hydroxide solution (2 M) until a pH of 5 was reached. A large excess of sodium perchlorate (1.00 g, 8.17 mmol) was then added, yielding a blue precipitate. This was dissolved by heating on a steam bath. Upon cooling, blue crystals of the product suitable for X-ray crystallography formed, which were filtered off, washed quickly with a small amount of cold methanol, and air-dried. Yield: 0.031 g, 76%. Anal. Calcd for $C_{20}H_{40}Cl_2CuN_6O_{10}$ ($[CuL^1](ClO_4)_2 \cdot 2H_2O$): C, 36.5; H, 6.1; N, 12.8. Found: C, 36.5; H, 5.8; N, 12.7. Electron microprobe: Cu and Cl uniformly present. UV−visible spectrum (water): λ_{max}, nm (ϵ_{max}) = 658 (101), 1144 (32). Selected IR bands (KBr, cm^{-1}): 3399 m, 3302 m, 3221 m, 2929 w, 1637 w, 1493 m, 1087 s, 627 s. Magnetic moment: μ_{eff} (290 K) = 1.90 μ_B.

Crystallography. Intensity data for a pink acicular crystal of **1**·H_2O, a pale purple-blue crystal of **4**, a green tabular crystal of **5**, and an aqua acicular crystal of **11** were measured on a Siemens/Nicolet R3m diffractometer using graphite-monochromated Mo Kα radiation for **1**·H_2O, **5**, and **11** and on a Rigaku AFC6S diffractometer using graphite-monochromated Mo Kα radiation for **4**. Cell constants were obtained from a least-squares refinement using the setting angles of 30 reflections ($10.12 < 2\theta < 29.30°$) for **1**·H_2O, 25 reflections ($26.86 < 2\theta < 32.96°$) for **4**, 25 reflections ($10.13 < 2\theta < 28.15°$) for **5**, and 25 reflections ($12.00 < 2\theta < 23.70°$) for **11**. The data were collected using the ω scan technique for **1**·H_2O, **5**, and **11** and the $\omega-2\theta$ scan technique for **4**. The intensities of three representative reflections were measured after every 197, 150, 50, and 297 reflections for **1**·H_2O, **4**, **5**, and **11**, respectively. A decay correction was applied in the case of **1**·H_2O, **5**, and **11**.[17] The data were corrected for Lorentz and polarization effects,[17] and an empirical absorption correction was applied in each case.[18] Crystal parameters and details of the data collection and refinement for **1**·H_2O, **4**, **5**, and **11** are summarized in Table 1.

The structures were solved by direct methods and expanded using standard Fourier routines in the TEXSAN software package.[19] All non-hydrogen atoms were refined with anisotropic thermal parameters in each case, except for those of the disordered DMF molecule in **5**, which were refined isotropically. In all cases, most hydrogens were included in calculated positions. Free-water hydrogens could not be located for **1**·H_2O, **4**, and **11**, but metal-bound-water hydrogens in **4** could be located from difference maps. All hydrogens were held fixed throughout subsequent refinement. The maximum and minimum peaks on the final difference Fourier map corresponded to 0.47 and −0.38 e $Å^{-3}$ for **1**·H_2O, 0.76 and −0.60 e $Å^{-3}$ for **4**, 0.89 and −0.76 e $Å^{-3}$ for **5**, and 0.53 and −0.52 e $Å^{-3}$ for **11**. Details of the solution and refinement of the structures are given in Table 1, selected bond lengths and angles in Tables 2−5, and ORTEP[20] views of the complexes in Figures 1−4.

(17) *XDISK: Data Reduction Program*, Version 4.20.2PC; Siemens Analytical X-Ray Instruments, Inc.: Madison, WI, 1989.
(18) Walker, N.; Stuart, D. *Acta Crystallogr., Sect. A* **1983**, *39*, 158.
(19) *teXsan: Crystal Structure Analysis Package*; Molecular Structure Corp.: Houston, TX, 1985 and 1992.
(20) Johnson, C. K. *ORTEP II*; Report ORNL-5136; Oak Ridge National Laboratory: Oak Ridge, TN, 1976.

Table 1. Crystallographic Data for $[NiL^1](ClO_4)_2 \cdot H_2O$ (**1**·H_2O), $[Ni_2L^3(H_2O)_6](ClO_4)_4 \cdot 3H_2O$ (**4**), $[Cu_2L^1Br_4] \cdot DMF$ (**5**), and $[CuL^1](ClO_4)_2 \cdot 2H_2O$ (**11**)

	1·H_2O	**4**	**5**	**11**
formula	$C_{20}H_{38}Cl_2N_6NiO_9$	$C_{20}H_{54}Cl_4N_6Ni_2O_{25}$	$C_{23}H_{43}Br_4Cu_2N_7O$	$C_{20}H_{40}Cl_2CuN_6O_{10}$
fw	636.16	1037.88	880.34	659.02
cryst syst	monoclinic	monoclinic	trigonal	monoclinic
space group	$P2_1/c$ (No. 14)	$P2_1/c$ (No. 14)	$P3_121$ (No. 152)	$P2_1/c$ (No. 14)
a, Å	9.212(3)	9.108(4)	10.889(5)	9.45(1)
b, Å	17.805(8)	25.857(5)		19.51(2)
c, Å	16.501(6)	17.524(2)	22.220(9)	15.10(1)
β, deg	103.36(3)	92.73(2)		96.93(8)
V, Å^3	2633(1)	4122(2)	2281(1)	2763(4)
Z	4	4	3	4
T, °C	−100	23	−60	−100
λ(Mo Kα), Å	0.710 69	0.710 69	0.710 69	0.710 69
crystal size, mm	0.44 × 0.16 × 0.12	0.28 × 0.20 × 0.20	0.18 × 0.14 × 0.05	not measd
ρ_{calcd}, g cm^{-3}	1.605	1.672	1.922	1.584
h, k, l ranges collected	$-10 \le h \le 0$, $-21 \le k \le 0$, $-18 \le l \le 19$	$0 \le h \le 10$, $0 \le k \le 30$, $-20 \le l \le 20$	$0 \le h \le 12$, $-12\ k \le 0$, $0 \le l \le 26$	$-11 \le h \le 0$, $0 \le k \le 23$, $-17 \le l \le 17$
transm factors	0.8527−0.8890	0.9443−1.0000	0.322−0.737	0.8132−1.0000
F(000)	1336	2160	1308	1380
μ, cm^{-1}	10.01	12.65	66.98	10.47
no. of data measd	5124	7961	4367	5328
no. of unique data	4807	7467	1595	5009
no. of obsd data [$I \ge 3.0\sigma(I)$]	3079	4162	996	2067
no. of params	343	514	157	352
R^a	0.038	0.062	0.051	0.063
$R_w{}^b$	0.037	0.075	0.042	0.046
GOF	1.97	2.96	1.95	1.73

^{a} $R = \sum(|F_o| - |F_c|/\sum|F_o|$. ^{b} $R_w = [\sum w(|F_o| - |F_c|)^2/\sum wF_o^2]^{1/2}$, where $w = [\sigma^2(F_o)]^{-1}$.

Table 2. Selected Bond Distances (Å) and Angles (deg) for $[NiL^1](ClO_4)_2 \cdot H_2O$ (**1**·H_2O)

Ni−N(1)	2.132(4)	Ni−N(2)	2.138(4)
Ni−N(3)	2.119(4)	Ni−N(4)	2.182(4)
Ni−N(5)	2.110(4)	Ni−N(6)	2.142(4)
N(1)−C(1)	1.497(5)	N(1)−C(6)	1.489(6)
N(1)−C(7)	1.497(5)	N(2)−C(2)	1.480(5)
N(2)−C(3)	1.475(5)	N(3)−C(4)	1.502(5)
N(3)−C(5)	1.482(6)	N(4)−C(14)	1.501(6)
N(4)−C(15)	1.482(6)	N(4)−C(20)	1.509(6)
N(5)−C(16)	1.494(6)	N(5)−C(17)	1.492(6)
N(6)−C(18)	1.480(6)	N(6)−C(19)	1.481(6)
C(1)−C(2)	1.508(6)	C(3)−C(4)	1.529(6)
C(5)−C(6)	1.532(6)	C(7)−C(8)	1.503(6)
C(8)−C(9)	1.387(6)	C(8)−C(13)	1.397(6)
C(9)−C(10)	1.394(7)	C(10)−C(11)	1.360(7)
C(11)−C(12)	1.401(7)	C(12)−C(13)	1.394(6)
C(13)−C(14)	1.499(6)	C(15)−C(16)	1.526(7)
C(17)−C(18)	1.517(7)	C(19)−C(20)	1.508(7)
N(1)−Ni−N(2)	82.4(1)	N(1)−Ni−N(3)	80.2(1)
N(1)−Ni−N(4)	103.6(1)	N(1)−Ni−N(5)	173.9(1)
N(1)−Ni−N(6)	103.3(1)	N(2)−Ni−N(3)	82.0(1)
N(2)−Ni−N(4)	105.3(1)	N(2)−Ni−N(5)	91.6(1)
N(2)−Ni−N(6)	169.7(1)	N(3)−Ni−N(4)	172.0(1)
N(3)−Ni−N(5)	97.6(1)	N(3)−Ni−N(6)	90.5(1)
N(4)−Ni−N(5)	79.3(1)	N(4)−Ni−N(6)	81.9(1)
N(5)−Ni−N(6)	82.4(1)		

Table 3. Selected Bond Distances (Å) and Angles (deg) for $[Ni_2L^3(H_2O)_6](ClO_4)_4 \cdot 3H_2O$ (**4**)

Ni(1A)−O(1A)	2.093(6)	Ni(1A)−O(2A)	2.118(6)
Ni(1A)−O(3A)	2.112(6)	Ni(1A)−N(1A)	2.139(6)
Ni(1A)−N(2A)	2.073(7)	Ni(1A)−N(3A)	2.047(7)
Ni(1B)−O(1B)	2.043(6)	Ni(1B)−O(2B)	2.098(6)
Ni(1B)−O(3B)	2.105(6)	Ni(1B)−N(1B)	2.093(6)
Ni(1B)−N(2B)	2.129(6)	Ni(1B)−N(3B)	2.058(7)
N(1A)−C(1A)	1.49(1)	N(1A)−C(6A)	1.49(1)
N(1A)−C(7A)	1.506(9)	N(2A)−C(2A)	1.50(1)
N(2A)−C(3A)	1.46(1)	N(3A)−C(4A)	1.50(1)
N(3A)−C(5A)	1.48(1)	C(1A)−C(2A)	1.51(1)
C(3A)−C(4A)	1.53(1)	C(5A)−C(6A)	1.53(1)
C(7A)−C(8A)	1.52(1)	C(8A)−C(9A)	1.36(1)
C(8A)−C(10A)	1.40(1)	C(9A)−C(10A)	1.39(1)
N(1B)−C(1B)	1.47(1)	N(1B)−C(6B)	1.49(1)
N(1B)−C(7B)	1.490(9)	N(2B)−C(2B)	1.49(1)
N(2B)−C(3B)	1.49(1)	N(3B)−C(4B)	1.48(1)
N(3B)−C(5B)	1.48(1)	C(1B)−C(2B)	1.50(1)
C(3B)−C(4B)	1.50(1)	C(5B)−C(6B)	1.48(1)
C(7B)−C(8B)	1.52(1)	C(8B)−C(9B)	1.40(1)
C(8B)−C(10B)	1.38(1)	C(9B)−C(10B)	1.38(1)
O(1A)−Ni(1A)−O(2A)	85.0(2)	O(1A)−Ni(1A)−O(3A)	88.4(2)
O(1A)−Ni(1A)−N(1A)	97.2(2)	O(1A)−Ni(1A)−N(2A)	177.5(3)
O(1A)−Ni(1A)−N(3A)	93.7(3)	O(2A)−Ni(1A)−O(3A)	88.4(3)
O(2A)−Ni(1A)−N(1A)	94.6(2)	O(2A)−Ni(1A)−N(2A)	97.0(2)
O(2A)−Ni(1A)−N(3A)	177.9(3)	O(3A)−Ni(1A)−N(1A)	173.9(3)
O(3A)−Ni(1A)−N(2A)	90.1(3)	O(3A)−Ni(1A)−N(3A)	93.3(3)
N(1A)−Ni(1A)−N(2A)	84.2(2)	N(1A)−Ni(1A)−N(3A)	83.8(3)
N(2A)−Ni(1A)−N(3A)	84.3(3)	O(1B)−Ni(1B)−O(2B)	85.8(2)
O(1B)−Ni(1B)−O(3B)	84.4(3)	O(1B)−Ni(1B)−N(1B)	94.2(2)
O(1B)−Ni(1B)−N(2B)	95.7(3)	O(1B)−Ni(1B)−N(3B)	178.8(3)
O(2B)−Ni(1B)−O(3B)	82.8(3)	O(2B)−Ni(1B)−N(1B)	179.1(3)
O(2B)−Ni(1B)−N(2B)	94.7(3)	O(2B)−Ni(1B)−N(3B)	95.3(3)
O(3B)−Ni(1B)−N(1B)	98.1(2)	O(3B)−Ni(1B)−N(2B)	177.5(3)
O(3B)−Ni(1B)−N(3B)	95.3(3)	N(1B)−Ni(1B)−N(2B)	84.4(3)
N(1B)−Ni(1B)−N(3B)	84.6(3)	N(2B)−Ni(1B)−N(3B)	84.6(3)

Results and Discussion

Preparation of Ligands. The three xylylene-bridged bis(tacn) ligands L^1−L^3 were prepared using adaptions to the method described by Zompa and co-workers[8] for the synthesis of similar alkylene-bridged bis(macrocycles). This involved reaction of 2 equiv of the tricyclic orthoamide derivative of tacn (1,4,7-triazatricyclo[5.2.1.0^{4,10}]decane) with 1,2-, 1,3-, and 1,4-bis(bromomethyl)benzene to afford bis(amidinium) salt intermediates, followed by base hydrolytic workup to yield the target compounds (Scheme 1). The ligands were conveniently isolated in good yields as their hexahydrobromide salts and their purities established by elemental analyses and proton and ^{13}C NMR spectroscopy.

Preparation and Characterization of Metal Complexes. Reaction of the hexahydrobromide salt of L^1 with ca. 3 molar equiv of $Ni(NO_3)_2 \cdot 6H_2O$ and subsequent addition of base yielded a pink-purple solution. Cation-exchange chromatography of this solution showed it to consist of a mixture of mononuclear and binuclear species, which were isolated as their perchlorate salts, $[NiL^1](ClO_4)_2$ (**1**) and $[Ni_2L^1(H_2O)_6](ClO_4)_4 \cdot$

Table 4. Selected Bond Distances (Å) and Angles (deg) for $[Cu_2L^1Br_4]\cdot$DMF (**5**)

Cu(1)−Br(1)	2.433(3)	Cu(1)−Br(2)	2.416(3)
Cu(1)−N(1)	2.23(1)	Cu(1)−N(2)	2.07(1)
Cu(1)−N(3)	2.05(1)	N(1)−C(1)	1.55(2)
N(1)−C(6)	1.44(2)	N(1)−C(7)	1.49(2)
N(2)−C(2)	1.47(2)	N(2)−C(3)	1.51(2)
N(3)−C(4)	1.48(2)	N(3)−C(5)	1.50(2)
C(1)−C(2)	1.50(2)	C(3)−C(4)	1.50(2)
C(5)−C(6)	1.50(2)	C(7)−C(8)	1.52(2)
C(8)−C(8a)	1.40(3)	C(8)−C(9)	1.37(2)
C(9)−C(10)	1.39(3)	C(10)−C(10a)	1.38(4)
Br(1)−Cu(1)−Br(2)	96.02(9)	Br(1)−Cu(1)−N(1)	101.5(3)
Br(1)−Cu(1)−N(2)	172.2(4)	Br(1)−Cu(1)−N(3)	91.2(4)
Br(2)−Cu(1)−N(1)	108.5(3)	Br(2)−Cu(1)−N(2)	88.6(4)
Br(2)−Cu(1)−N(3)	164.9(4)	N(1)−Cu(1)−N(2)	82.9(5)
N(1)−Cu(1)−N(3)	82.9(5)	N(2)−Cu(1)−N(3)	82.9(5)

Table 5. Selected Bond Distances (Å) and Angles (deg) for $[CuL^1](ClO_4)_2\cdot 2H_2O$ (**11**)

Cu−N(1)	2.129(8)	Cu−N(2)	2.023(8)
Cu−N(3)	2.438(8)	Cu−N(4)	2.442(8)
Cu−N(5)	2.053(7)	Cu−N(6)	2.109(8)
N(1)−C(1)	1.50(1)	N(1)−C(6)	1.50(1)
N(1)−C(7)	1.50(1)	N(2)−C(2)	1.47(1)
N(2)−C(3)	1.47(1)	N(3)−C(4)	1.47(1)
N(3)−C(5)	1.49(1)	N(4)−C(14)	1.48(1)
N(4)−C(15)	1.47(1)	N(4)−C(20)	1.49(1)
N(5)−C(16)	1.49(1)	N(5)−C(17)	1.49(1)
N(6)−C(18)	1.50(1)	N(6)−C(19)	1.47(1)
C(1)−C(2)	1.52(1)	C(3)−C(4)	1.53(1)
C(5)−C(6)	1.52(1)	C(7)−C(8)	1.52(1)
C(8)−C(9)	1.41(1)	C(8)−C(13)	1.36(1)
C(9)−C(10)	1.38(1)	C(10)−C(11)	1.36(1)
C(11)−C(12)	1.39(1)	C(12)−C(13)	1.39(1)
C(13)−C(14)	1.51(1)	C(15)−C(16)	1.52(1)
C(17)−C(18)	1.51(1)	C(19)−C(20)	1.52(1)
N(1)−Cu−N(2)	83.6(3)	N(1)−Cu−N(3)	76.7(3)
N(1)−Cu−N(4)	99.2(3)	N(1)−Cu−N(5)	172.6(3)
N(1)−Cu−N(6)	105.0(3)	N(2)−Cu−N(3)	79.2(3)
N(2)−Cu−N(4)	120.5(3)	N(2)−Cu−N(5)	90.7(3)
N(2)−Cu−N(6)	160.2(3)	N(3)−Cu−N(4)	159.6(3)
N(3)−Cu−N(5)	107.0(3)	N(3)−Cu−N(6)	85.5(3)
N(4)−Cu−N(5)	79.6(3)	N(4)−Cu−N(6)	76.3(3)
N(5)−Cu−N(6)	82.0(3)		

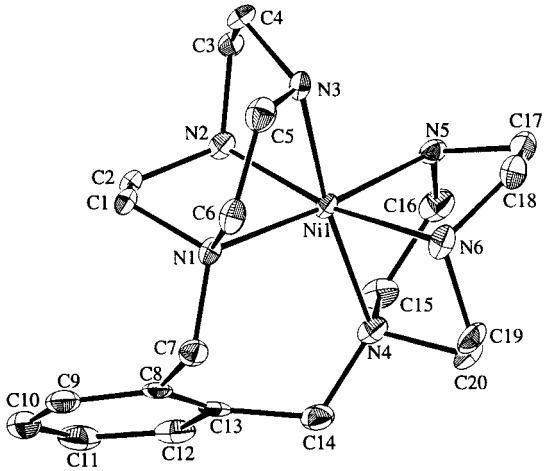

Figure 1. ORTEP[20] plot of the molecular cation in $[NiL^1](ClO_4)_2\cdot H_2O$ (**1**·H_2O) with the atomic labeling scheme (thermal ellipsoids are drawn at 50% probablility).

$4H_2O$ (**2**), respectively. Thus, an important feature of the ligand L^1 is its ability to behave as either a hexadentate ligand, coordinating to one nickel(II) center, or as a bis(tridentate) ligand, coordinating to two nickel(II) centers. This behavior is in contrast to that of the ethylene-linked bis(tacn) macrocycle, where only the mononuclear nickel(II) sandwich complex can

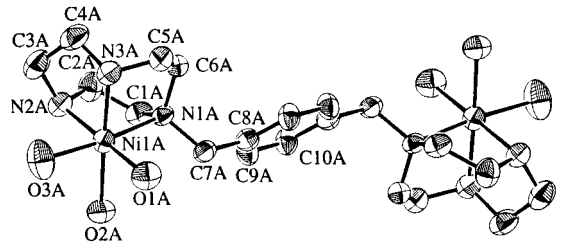

Figure 2. ORTEP[20] plot of the molecular cation in $[Ni_2L^3(H_2O)_6](ClO_4)_4\cdot 3H_2O$ (**4**) with the atomic labeling scheme (thermal ellipsoids are drawn at 50% probablility).

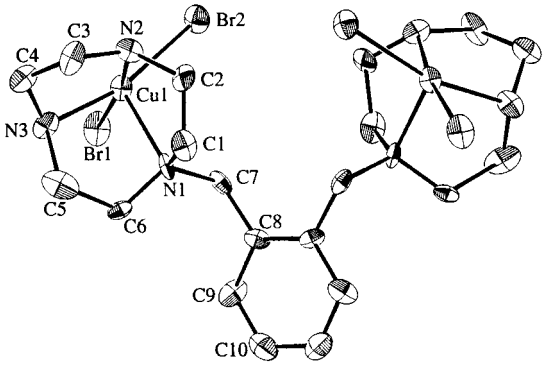

Figure 3. ORTEP[20] plot of $[Cu_2L^1Br_4]\cdot$DMF (**5**) with the atomic labeling scheme (thermal ellipsoids are drawn at 50% probablility).

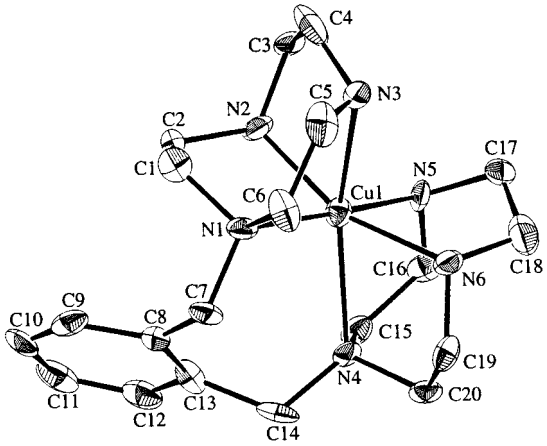

Figure 4. ORTEP[20] plot of the molecular cation in $[CuL^1](ClO_4)_2\cdot 2H_2O$ (**11**) with the atomic labeling scheme (thermal ellipsoids are drawn at 50% probablility).

be isolated.[2,21] Similar reactions of the ligands L^2 and L^3 with excess Ni^{2+} ions yielded only the binuclear products, $[Ni_2L^2(H_2O)_6](ClO_4)_4$ (**3**) and $[Ni_2L^3(H_2O)_6](ClO_4)_4\cdot 3H_2O$ (**4**), respectively. In these cases, the *m*- and *p*-xylylene spacer groups between the tacn macrocycles prevent simultaneous coordination of both rings to one metal center.

Addition of ca. 3 molar equiv of $CuBr_2$ to aqueous solutions of the hexahydrobromide salts of ligands L^1−L^3 and subsequent addition of base produced dark blue solutions from which green solids were readily isolated. Recrystallization of these from water/DMF yielded complexes of composition $[Cu_2LBr_4]\cdot x$DMF (**5**, L = L^1, $x = 1$; **6**, L = L^2, $x = 0$; **7**, L = L^3, $x = 0$). Binuclear copper(II) complexes with the composition $[Cu_2L(H_2O)_4](ClO_4)_4\cdot xH_2O$ were also crystallized, following cation-exchange chromatography (**8**, L = L^1, $x = 5$; **9**, L = L^2, $x = 4$; **10**, L = L^3, $x = 5$).

The mononuclear sandwich complex $[CuL^1](ClO_4)_2\cdot 2H_2O$ (**11**) was produced by addition of 1 molar equiv of $Cu(NO_3)_2\cdot 3H_2O$ to an aqueous solution of $L^1\cdot 6HBr\cdot 1.5H_2O$, adjustment

(21) Graham, B.; Spiccia, L. Unpublished work.

Scheme 1

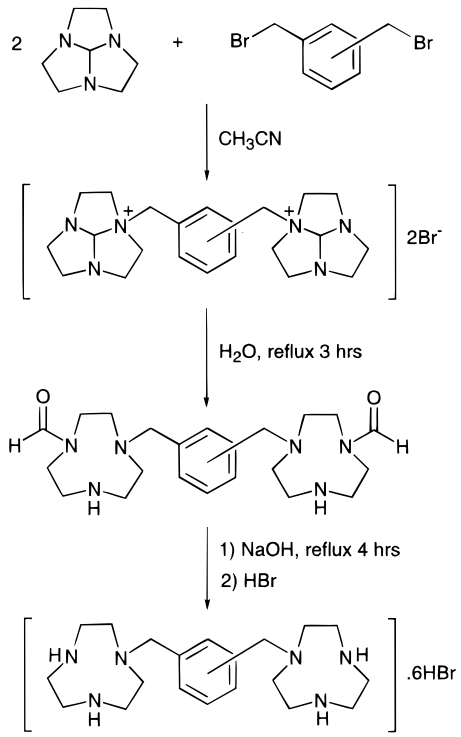

of the pH to 5, and addition of excess sodium perchlorate. Thus, the *o*-xylylene-linked bis(tacn) ligand (L^1) shows variation in its mode of coordination, viz. forming binuclear complexes in the presence of excess metal ion but preferring to form mononuclear complexes when low metal ion/ligand ratios are used.

Analytical data for each of the nickel(II) and copper(II) complexes were consistent with the given compositions. The IR spectra for all complexes showed bands due to N−H stretches in the 3200−3350 cm^{-1} region and, for complexes **1**−**4** and **8**−**11**, bands due to the perchlorate counterions at ca. 1090 and 625 cm^{-1}. The room-temperature magnetic moments of the nickel(II) complexes (2.9−3.0 μ_B per nickel(II) center) were in the typical range for octahedral nickel(II) complexes,[22] while those for the copper (II) complexes (1.8−1.9 μ_B per copper(II) center) were atypical.[23] Variable-temperature magnetism studies of the binuclear complex **4** showed no evidence of spin−spin coupling, as has been observed for series of related copper(II) complexes.[15,16] The binuclear complexes **2**, **3**, and **5**−**10** would likewise be expected to show little, if any, magnetic exchange interaction occurring between the metal centers, due to the absence of bridging groups capable of mediating such interaction.

Crystal Structures. The molecular structure of compound **1**·H_2O consists of discrete mononuclear $[NiL^1]^{2+}$ cations (Figure 1), perchlorate anions, and waters of crystallization. The geometry about the nickel(II) center is distorted octahedral with the two tacn moieties of the ligand coordinated to two faces of the octahedron. The intra-ring N_{cis}−Ni−N_{cis} "bite" angles (79−83°) are all well below the 90° expected for an idealized octahedral structure due to the constraints imposed by three edge-sharing, five-membered chelate rings of the tacn moiety. Distortion from an idealized octahedral structure is also evident from the fact that there is a dihedral angle of 9.0° between the plane passing through N(1), N(2), and N(3) and the plane passing through N(4), N(5), and N(6). The observed reduction in the *trans* angles about the nickel(II) from 180° (viz. N(2)−Ni−N(6) = 169.7(1)°) further highlights this distortion. In addition, the Ni−N(4) bond (2.182(4) Å) is significantly longer than the remaining Ni−N bonds (2.110(4)−2.142(4) Å), probably due to the geometric constraints imposed by the *o*-xylylene bridge. The benzene ring of the bridge is tilted toward the tacn ring containing N(1), N(2), and N(3), thus drawing the N(4) atom away from the nickel(II) center. A more dramatic example of this type of effect is found in $[Ni(L^4)_2]^{2+}$ (where L^4 = 1-benzyl-1,4,7-triazacyclononane),[24] in which the bonds to the two tertiary nitrogens attached to the pendant benzyl groups are substantially longer than the other four Ni−N bonds (viz., ca. 2.25 Å vs 2.09−2.12 Å). In sharp contrast, the Ni−N bond lengths in $[Ni(tacn)_2]^{2+}$ are in the 2.09−2.12 Å range and reflect the more symmetric coordination environment provided by the secondary nitrogens of the unsubstituted tacn macrocycle.[25]

Crystals of **11** are composed of mononuclear $[CuL^1]^{2+}$ cations (Figure 4), perchlorate anions, and waters of crystallization. The copper(II) center is six-coordinate, sandwiched by the two tacn rings of the ligand L^1. The coordination sphere displays the expected Jahn−Teller distortion imposed by the d^9 copper(II) ion, with two long Cu−N bonds (2.438(8) and 2.442(8) Å) and four short Cu−N bonds (2.023(8)−2.129(8) Å). Similar distorted d^9 CuN_6 coordination polyhedra are observed in the structures of $[Cu(tacn)_2]^{2+}$,[26] $[Cu(dien)_2]^{2+}$ (where dien = diethylenetriamine),[27] and $[Cu(terpy)_2]^{2+}$ (where terpy = 2,2′:6′,2″-terpyridine),[28] although shorter axial bonds are observed in $[Cu(tacn)_2]^{2+}$. Distortion due to the geometric constraints imposed by the *o*-xylylene bridge is evident from the fact that there is a dihedral angle of 9.5° between the plane passing through N(1), N(2), and N(3) and the plane passing through N(4), N(5), and N(6). As in complex **1**·H_2O, the benzene ring of the bridge is tilted toward the tacn ring containing N(1), N(2), and N(3).

It is interesting to compare the degree of trigonal distortion in the two mononuclear complexes. For **1**·H_2O, if a line passing through the centroid of N(1), N(2), and N(3) and the centroid of N(4), N(5), and N(6) is considered as a pseudo-C_3 axis, the trigonal twist angles deviate by 7.0 ± 2.1° from the value of 60° expected for an octahedron. For $[Ni(tacn)_2]^{2+}$ the twist angles deviate by 3.8 ± 0.8° from the octahedral value. Thus, although the trigonal distortion, as shown by the N−Ni−N angles, is large in both $[NiL^1]^{2+}$ and $[Ni(tacn)_2]^{2+}$ [25] (due to elongation along the C_3 axis) the trigonal twist distortion is relatively small. On the other hand, the degree of trigonal twist distortion is much greater in the copper(II) complex **11** than in these nickel(II) complexes; viz., the trigonal twist angles deviate by 20.3 ± 2.1° from the octahedral value.

Crystals of compound **4** are composed of binuclear $[Ni_2L^3(H_2O)_6]^{4+}$ cations, perchlorate anions, and waters of crystallization. Two slightly different forms of the cation are present in the unit cell, one of which is illustrated in Figure 2. The nickel(II) centers are each surrounded by a distorted octahedral array of one *fac*-coordinated triamine ring and three water molecules. The two nickel(II) centers in each of the cation units are oriented away from one another so that the cations display *anti* conformations and are centrosymmetric about the midpoint

(22) Sacconi, L.; Mani, F.; Bencini, A. In *Comprehensive Coordination Chemistry*; Wilkinson, G., Gillard, R. D., McCleverty, J. A., Eds.; Pergamon Press: Oxford, England, 1987; Vol. 5, p 1.
(23) Hathaway, B. J. In *Comprehensive Coordination Chemistry*; Wilkinson, G., Gillard, R. D., McCleverty, J. A., Eds.; Pergamon Press: Oxford, England, 1987; Vol. 5, p 533.
(24) Blake, A. J.; Fallis, I. A.; Parsons, S.; Ross, S. A.; Schröder, M. *J. Chem. Soc., Dalton Trans.* **1996**, 525.
(25) Zompa, L. J.; Margulis, T. N. *Inorg. Chim. Acta* **1978**, *28*, L157.
(26) Beveridge, A. D.; Lavery, A. J.; Walkinshaw, M. D.; Schröder, M. *J. Chem. Soc., Dalton Trans.* **1987**, 373.
(27) Stephens, F. S. *J. Chem. Soc. A* **1969**, *883*, 2233.
(28) Mathew, M.; Palenik, G. J. *J. Coord. Chem.* **1971**, *1*, 243.

of the *p*-xylylene bridge. This conformation is probably favored by steric and electrostatic factors. As a result of the open structure adopted, long intramolecular Ni···Ni separations of 11.68 Å are observed in both of the cation forms. The Ni−N(secondary amine) distances (2.047(7)−2.093(6) Å) are significantly shorter than the Ni−N(tertiary amine) distances (2.129(6) and 2.139(6) Å) and reflect the stronger binding properties of secondary nitrogens. As was the case for **1**·H_2O, the intra-ring N_{cis}−Ni−N_{cis} bond angles are all below the 90° expected for an ideal octahedral geometry. The N_{trans}−Ni−N_{trans} angles in **4**, however, are on average closer to the ideal 180° (174−179°) than those in **1**·H_2O (170−174°). This can be attributed to the more flexible coordination sphere in **4** compared with that in **1**·H_2O, where additional steric constraints are introduced by sandwiching the nickel(II) center between the two tacn macrocycles.

The molecular structure of compound **5** consists of neutral $[Cu_2L^1Br_4]$ molecules (Figure 3) and noncoordinated DMF molecules that are disordered. A 2-fold axis bisecting the *o*-xylylene bridge divides the binuclear unit into two halves, with the copper(II) centers separated by a distance of 7.21 Å. These reside in distorted square pyramidal environments with basal planes defined by two Br atoms and two secondary amine N atoms; the apical position, in each case, is occupied by the bridgehead N(1) amine atom. The degree of trigonal distortion from ideal square pyramidal geometry may be defined using the geometric parameter $\tau = [(\theta - \phi)/60] \times 100$, where θ and ϕ represent the largest and second largest basal angles, respectively. According to Addison,[29] an ideal square pyramid has a τ value of 0%, while τ becomes 100% for a perfect trigonal bipyramid structure. The relevant angles in **5**, $\theta = 172.2(2)°$ and $\phi = 164.9(4)°$, yield a τ value of 12%, which indicates a geometry close to regular square pyramidal. The mean deviation of the basal atoms from their least-squares plane is 0.06 Å, with the copper(II) displaced 0.18 Å from the plane in the direction of N(1). The two Cu−Br separations are equivalent, whereas the Cu−N distances in the basal plane (average 2.06 Å) are shorter than the Cu−N(apical) distance of 2.23(1) Å. Apart from this, the tridentate mode of coordination of L^1 about each copper(II) parallels that observed in the binuclear nickel(II) complex **4**.

A comparison of the structures of copper(II) complexes of tacn and binucleating derivatives of tacn, viz. the mononuclear complexes such as $[Cu(tacn)Cl_2]$[30] and $[Cu(tacn)Br_2]$[31] and the binuclear complexes such as **5**, $[Cu_2L^5Cl_4]$·$2H_2O$ (where L^5 = 1,3-bis(1,4,7-triazacyclonon-1-yl)propane),[8] and $[Cu_2L^6Cl_4]$ (where L^6 = 1,4-bis(1,4,7-triazacyclonon-1-yl)butane),[8] reveals similar geometries. In each case, the geometry about copper(II) is best described as distorted square pyramidal with two nitrogen and two halide donors forming the basal plane and a nitrogen donor occupying the apical position. In the complexes of the binucleating bis(tacn) macrocycles, the two secondary nitrogens are in the basal plane and the tertiary nitrogen is in the axial position. The similarities in these structures are highlighted by the fact that the two bromo complexes, $[Cu(tacn)Br_2]$ and **5**, have virtually identical Cu−N and Cu−halide distances, a feature also observed in the three chloro complexes. The stabilization of the distorted square pyramidal geometry over trigonal bipyramidal geometry indicates that the tacn macrocycle is better accommodated on one of the four smaller faces of an axially elongated square pyramid than on a larger face of a trigonal bipyramid.

Table 6. Electronic Spectral Data for Nickel(II) Complexes of 1,4,7-Triazacyclononane-Derived Ligands

complex	solvent	λ_{max}, nm (ϵ_{max})	chromophore
1	MeCN	340 (sh), 359 (7), 538 (7), 625 (sh), 840 (sh), 912 (16)	NiN_6
$[Ni(tacn)_2]^{2+}$ [a]	water	308 (12), 505 (5), 800 (7), 870 (sh)	NiN_6
$[Ni(L^4)_2]^{2+}$ [b]	MeCN	390 (18), 532 (6), 840 (sh), 961 (11)	NiN_6
$[NiL^7]^{2+}$ [c]	water	363 (16), 516 (18), 848 (31), 917 (31)	NiN_6
2	water	356 (13), 578 (9), 775 (sh), 978 (30)	NiN_3O_3
3	water	358 (11), 579 (8), 775 (sh), 972 (32)	NiN_3O_3
4	water	357 (11), 581 (9), 775 (sh), 973 (35)	NiN_3O_3
$[Ni(tacn)(H_2O)_3]^{2+}$ [a]	water	334 (5), 575 (4), 877 (sh), 962 (14)	NiN_3O_3

[a] Reference 34. [b] Reference 24; L^4 = 1-benzyl-1,4,7-triazacyclononane. [c] Reference 2; L^7 = 1,2-bis(1,4,7-triazacyclonon-1-yl)ethane.

Electronic Spectra of Metal Complexes. Electronic spectral data for the nickel(II) complexes **1**−**4** are summarized in Table 6 together with those for related nickel(II) complexes. Each complex shows three absorption maxima typical of octahedral nickel(II) complexes: spin-allowed $^3A_{2g}$−$^3T_{2g}$ (950−800 nm), $^3A_{2g}$−$^3T_{1g}$(F) (550−500 nm), and $^3A_{2g}$−$^3T_{1g}$(P) (300−400 nm) transitions.[32,33] The low-energy band is asymmetric (or has a shoulder) in each case due to the presence of a weaker spin-forbidden $^3A_{2g}$−^1E_g transition. For **1**, the intermediate- and high-energy bands also display distinct splittings, a reflection of the low symmetry of the ligand field. The 10*Dq* value for $[NiL^1]^{2+}$ of 11 000 cm^{-1} (taken from lowest energy transition at 912 nm) is intermediate between those for $[Ni(L^4)_2]^{2+}$ (where L^4 = 1-benzyl-1,4,7-triazacyclononane) (10*Dq* = 10 400 cm^{-1}) [24] and $[Ni(tacn)_2]^{2+}$ (10*Dq* = 12 500 cm^{-1}).[34] In $[Ni(L^4)_2]^{2+}$, the steric bulk of the benzyl group in the L^4 ligand prevents the Ni−N bonds from approaching the optimum length of 2.08 Å,[35] resulting in a substantially weaker ligand field when compared with that of the unsubstituted tacn. The weaker ligand field of L^1 relative to tacn can be attributed to steric constraints, introduced by the *o*-xylylene group linking the two tacn compartments and the conversion of a secondary nitrogen into a tertiary nitrogen. Both of these factors combine to reduce the binding ability of the bis(macrocycle) as is evident from the Ni−N distances. Notably, one of the Ni−N(tertiary) distances is substantially longer than all the other Ni−N distances in $[NiL^1]^{2+}$. The similar and relatively low values of the molar extinction coefficients of $[NiL^1]^{2+}$ and $[Ni(tacn)_2]^{2+}$ indicate that the degree of trigonal distortion of the geometry around nickel(II) in these two complexes is lower than in $[NiL^7]^{2+}$ (where L^7 = 1,2-bis(1,4,7-triazacyclonon-1-yl)ethane),[2] which exhibits more intense bands. This is the case even though the band positions indicate that the ligand field strengths of the *o*-xylylene- and ethylene-linked bis(tacn) ligands, L^1 and L^7, respectively, are very similar. In going from $[NiL^1]^{2+}$ to the $[Ni_2L(OH_2)_6]^{4+}$ series of compounds, where L = L^1, L^2, or L^3, the replacement of three nitrogen donors in the NiN_6 coordination sphere by oxygen donors, from the weaker end of the spectrochemical series, causes a general red shift in the bands.

(29) Addison, A. W.; Rao, T. N.; Reedijk, J.; van Rijn, J.; Verschoor, G. C. *J. Chem. Soc., Dalton Trans.* **1984**, 1349.
(30) Schwindinger, W. F.; Fawcett, T. G.; Lalancette, R. A.; Potenza, J. A.; Schugar, H. J. *Inorg. Chem.* **1980**, *19*, 1379.
(31) Bereman, R. D.; Churchill, M. W.; Schaber, P. M.; Winkler, M. E. *Inorg. Chem.* **1979**, *18*, 3122.
(32) Lever, A. B. P. *Inorganic Electronic Spectroscopy*; Elsevier: Amsterdam, 1968.
(33) Robinson, M. A.; Curry, J. D.; Busch, D. H. *Inorg. Chem.* **1963**, *2*, 1178.
(34) Yang, R.; Zompa, L. J. *Inorg. Chem.* **1976**, *15*, 1499.
(35) Hancock, R. D. *Prog. Inorg. Chem.* **1989**, *37*, 187.

Table 7. Electronic Spectral Data for Copper(II) Complexes of 1,4,7-Triazacyclononane-Derived Ligands

complex	solvent	λ_{max}, nm (ϵ_{max})	chromophore
8	water	655 (79), 1056 (35)	CuN_3O_2
9	water	645 (72), 1044 (35)	CuN_3O_2
10	water	649 (70), 1050 (35)	CuN_3O_2
$[Cu(tacn)(H_2O)_2]^{2+}$ [a]	water	654 (40), 1075 (13)	CuN_3O_2
$[Cu_2L^5(H_2O)_4]^{4+}$ [b]	water	647 (102), 1060 (41)	CuN_3O_2
$[Cu_2L^6(H_2O)_4]^{4+}$ [c]	water	645 (112), 1055 (50)	CuN_3O_2
11	water	658 (101), 1144 (32)	CuN_6
$[Cu(tacn)_2]^{2+}$ [d]	water	620 (360), 1235 (48)	CuN_6[e]
$[CuL^5]^{2+}$ [b]	water	644 (53), 1060 (15)	CuN_6
$[CuL^6]^{2+}$ [c]	water	653 (53), 1075 (17)	CuN_6
$[CuL^7]^{2+}$ [f]	*g*	646 (126)	CuN_6

[a] Reference 31. [b] Reference 8; L^5 = 1,3-bis(1,4,7-triazacyclonon-1-yl)propane. [c] Reference 8; L^6 = 1,4-bis(triazacyclonon-1-yl)butane. [d] Reference 34. [e] Studies suggest that partial dissociation and solvation occur in solution; see ref 34. [f] Reference 2; L^7 = 1,2-bis(1,4,7-triazacyclonon-1-yl)ethane. [g] Not reported.

As might be anticipated from the similarities in ligands L^1, L^2, and L^3, the positions of the bands for complexes **2**−**4** indicate that these ligands have very similar ligand field strengths. The intensities of these bands further suggest a comparable level of distortion from octahedral geometry for each complex.

Electronic spectroscopic data for the copper(II) complexes **8**−**11** are summarized in Table 7 together with data for related five-coordinate square pyramidal copper(II) complexes possessing CuN_3O_2 chromophores or six-coordinate octahedral copper(II) complexes possessing CuN_6 chromophores. Each complex shows two weak d−d transitions centered at ca. 650 and 1050 nm, in agreement with a $(d_{x^2-y^2})^1$ electronic ground-state of a copper(II) ion in either a square pyramidal or a tetragonally distorted octahedral geometry,[23] for which $d_{z^2} \rightarrow d_{x^2-y^2}$ and d_{yz}, $d_{xz} \rightarrow d_{x^2-y^2}$ transitions are expected. The band at ca. 650 nm is broad and asymmetric showing evidence of a $d_{xy} \rightarrow d_{x^2-y^2}$ transition, which is expected for square pyramidal or tetragonally distorted copper(II) complexes. Interpretation of the electronic spectra of $[Cu(tacn)_2]^{2+}$ and the mononuclear copper(II) complexes of the bis(tacn) ligands, where an N_6 donor set surrounds the copper(II) center, is complicated by evidence[26] that $[Cu(tacn)_2]^{2+}$ partially dissociates in solution, forming solvated bis(macrocyclic) products, $[Cu(tacn)_2S_n]^{2+}$ (S = solvent molecule), in which one tacn ligand acts as a mono- or bidentate ligand, and mono(macrocyclic) products of the form $[Cu(tacn)S_n]^{2+}$. The spectra of the sandwich copper(II) complexes of the bis(tacn) macrocycles, including that of the *o*-xylylene-linked complex reported here, are similar to each other and different from that of $[Cu(tacn)_2]^{2+}$, indicating either no dissociation or a similar degree of dissociation in solution, e.g. formation of a square pyramidal complex with an CuN_5 chromophore through dissociation of an axial ligand.

Electron Spin Resonance Spectra of Copper(II) Complexes. X-band ESR spectra of the copper(II) complexes **8**−**11** were measured on frozen DMF solutions at 77 K. Each spectrum shows a very strong signal at ca. 3100 G, typical of that found for mononuclear copper(II) complexes with nuclear spin $^3/_2$,[23] suggesting the absence of any interaction between the copper(II) centers in dilute solution: three of the four expected hyperfine signals are displayed, with the fourth being hidden under the $g_\perp$ line. The spectra were successfully simulated using a combination of Gaussian and Lorentzian line shapes in equal proportion. The parameters obtained (Table 8) are typical of square pyramidal or tetragonally distorted octahedral copper(II) complexes, for which $g_\parallel > g_\perp > 2$,[23] consistent with the geometry found in the crystal structures of copper(II) complexes of tacn and binucleating derivatives of tacn, viz. the mononuclear complexes such as **11**, $[Cu(tacn)Cl_2]$,[30] and $[Cu(tacn)Br_2]$[31] and the binuclear complexes such as **5**, $[Cu_2L^5Cl_4]\cdot 2H_2O$ (where L^5 = 1,3-bis(1,4,7-triazacyclonon-1-yl)propane),[8] and $[Cu_2L^6Cl_4]$ (where L^6 = 1,4-bis(1,4,7-triazacyclonon-1-yl)butane).[8]

Table 8. ESR Parameters for Copper(II) Complexes **8**−**11** in Frozen DMF Solution (77 K)

complex	g_{xx}	g_{yy}	g_{zz}	$10^{-4}A_{xx}$, cm^{-1}	$10^{-4}A_{yy}$, cm^{-1}	$10^{-4}A_{zz}$, cm^{-1}
8	2.026	2.084	2.280	0	0	170
9	2.059	2.059	2.285	0	19	171
10	2.059	2.059	2.285	0	19	171
11	2.046	2.046	2.230	0	24	171

Conclusion

The coordination modes of *o*-, *m*-, and *p*-xylylene-linked bis(tacn) macrocycles have been examined through the study of their nickel(II) and copper(II) complexes. The impetus for these investigations is the potential application of such complexes as receptors for substrates with two coordinating groups separated by a distance complementary to the metal−metal separation. It is clear from the present study that the metal−metal distance in the solid state can be varied between ca. 7 and 12 Å by changing the ligand. Of course, the presence of four carbon−carbon single bonds in the bridging units of L^1, L^2, and L^3 means that a range of conformations, and hence metal−metal separations, will be accessible to each complex in solution. Reduction of the metal−metal distances to ca. 3.5 Å, together with freezing out of the rotational degrees of freedom of the complexes, may be possible through the introduction of exogenous bridges between the metal centers. In order to establish the ability of the complexes described in this paper to selectively bind particular substrates, complexation with a variety of substrates, e.g. imidazole, bis(imidazoles), phosphates, and phosphate esters, is currently under investigation.

Acknowledgment. This work was supported by the Australian Research Council. B.G. is the recipient of an Australian Postgraduate Award.

Note Added in Proof. Following submission of this paper, the independent syntheses of the xylylene-bridged bis(tacn) ligands, together with the structure and properties of a binuclear μ-hydroxy-bridged copper(II) complex of the *m*-xylylene-bridged ligand, were communicated: Farrugia, L. J.; Lovatt, P. A.; Peacock, R. D. *J. Chem. Soc., Dalton Trans.* **1997**, 911.

Supporting Information Available: Listings of atomic coordinates and equivalent isotropic displacement parameters, anisotropic displacement parameters, hydrogen coordinates and isotropic displacement parameters, all bond distances, and all bond angles and figures showing experimental and simulated X-band ESR spectra (52 pages). Ordering information is given on any current masthead page.

IC970642W